Supporting Information

Synergetic Enhancement of Polysulfide Chemisorption and Electrocatalysis over Bicontinuous MoN@N-Rich Carbon Porous Nano-Octahedrons for Li-S Batteries

Peng Wang, Na Li, Zhian Zhang, Bo Hong, Jie Li, Kai Zhang, Keyu Xie*, Yanqing Lai**

Dr. P.Wang, Prof. Z.A. Zhang, Dr. B.Hong, Prof. J. Li, Dr. K. Zhang, Prof. Y.Q. Lai

School of Metallurgy and Environment, Central South University, Changsha 410083, China

E-mail: zhangzhian@csu.edu.cn; laiyanqing@csu.edu.cn

Prof. K. Y. Xie

State Key Laboratory of Solidification Processing, Center for Nano Energy Materials, School of Materials Science and Engineering, Northwestern Polytechnical University and Shaanxi Joint Laboratory of Graphene (NPU), Xi'an 710072, China.

E-mail: kyxie@nwpu.edu.cn

Experiment

Preparation of NENU-5:

Solution A: The Cu-based NENU-5 POMOFs were used as the precursor for the synthesis of MoN-CN nano-octahedrons. The MENU-5 was synthesized by method as described as previous report [1]. Specifically, 0.7355 g of L-glutamic acid, 3 g of phosphomolybdic acid hydrate and 2 g of copper acetate monohydrate are dissolved into 500 mL deionized water (DI) and stirred for 0.5 h. Solution B: 1.4 g of 1, 3, 5-benzenetricarboxylic acid was dissolved in 400 mL of ethanol. Solution B was introduced into solution A under stirring under room temperature under continuous string for 14 h. The green precipitate was rinsed with DI, and finally dried at 70 °C overnight.

Preparation of Porous MoO_2-C Nano-Octahedrons:

The green NENU-5 nano-octahedrons were annealed at 650 °C for 3 h under an Ar atmosphere with a heating ramp of 2 °C min^{-1}. The as-obtained was denoted as MoO_2-C-Cu. Then, the black sample was dispersing into 0.1 M $FeCl_3$ aqueous solution under string for 12 h to remove the copper particles. The resulting porous MoO_2-C nano-octahedrons was washed with DI and followed by vacuum drying at 70 °C for 12 h. As a control experiment, MoO_2-C nano-octahedron was treated with 0.2 M diluted hydrochloric acid and denoted C nano-octahedron.

Preparation of Porous MoN-NC Nano-Octahedrons:

The MoO_2-C and C nano-octahedrons were annealed at 650 °C for 6 h ammonia flow and the heating rate was 2 °C min^{-1}. Finally, the porous MoN-NC and CN nano-octahedrons were obtained. As a control experiment, bulk MoO_2 was annealed by the same procedure to prepare the bulk MoN material.

Preparation of S/MoN-NC composites

Sulfur encapsulation was performed via a melt-diffusion method. A mixture of sulfur (77 wt %) with MoN-NC composites was hand-milled for 20 min and then transferred to an autoclave and heated at 155 °C for 12 h. Upon cooling, the final materials were collected as 77S/MoN-NC. The 77S/MoN and 77S/NC composites were prepared via the same procedure as above.

Preparation of Li_2S_6 Solution:

The Li_2S_6 solution was prepared by dissolving lithium sulfide (46 mg) and sublimed sulfur (224 mg) in a molar ratio of 1:7 in 5 mL in 1,2-dimethoxyethane (DME, 99.5%, Alfa Aesar), and 1,3-dioxolane (DOL, 99.5%, Alfa Aesar) (1:1 ratio, by volume).

The morphology analyses were conducted with TEM (Nova Nano SEM 230) and TEM (Tecnai G2 20ST) coupled with an attached energy dispersive X-ray spectroscopy (EDS). Powder X-ray diffraction (XRD, Rigaku 3014) were characterized with Cu-Kα source. The sulfur content was confirmed by TGA analysis (Netzsch, STA 449C) under N_2 flow at a heating rate of 10 °C/min. The N_2 adsorption measurements were performed on ASAP 2460 analyzer (Micromeritics, USA) at 77 K. The chemical state of elements in composites was tested on X-ray photo-electron spectroscopy (XPS, ESCA LAB 250Xi).

Electrochemical Measurement:

To prepare the working electrode, a slurry was obtained by mixing and stirring the as-prepared composites, conductive carbon black and polyvinyldifluoride (PVDF) with the mass ratio of 8:1:1 in N-methyl-2-pyrrolidone, respectively. Then, the slurry was spread onto Al current collector and dried under vacuum at 60 °C for 12 h in vacuum for 10 h. The sulfur loading was controlled at 1.9–4.9 mg cm^{-2}. The coin-type cells (2032) were assembled with metallic Li as the counter electrodes and Celgard 2400 as a separator. The electrolyte was consisted of 1.0 m lithium bis(trifluoromethanesulfonyl) imide (LiTFSI) in 1, 3-dioxolane (DOL) and 1,2-dimethoxyethane (DME) (v/v, 1:1) with 2 % $LiNO_3$ as the additive. The volume of the electrolyte used in each cell was 30–50 μL, and the electrolyte-to-sulfur (E/S) ratio was about 15–20 μL mg^{-1}. Discharge/charge tests were carried out between 1.7 and 2.8 V (vs Li/Li^+) at various C rates (1 C = 1675 mA h g^{-1}) with LAND-CT2001A instruments (Wuhan Jinnuo, China). CV and EIS measurements were performed on electrochemical workstation (Solartron 1470E battery test) with a scan rate of 0.1 mV s^{-1}. In addition, EIS were performed using electrochemical workstation (Solartron 1470E battery test) in the frequency range between 10 mHz and 100 kHz.

Calculation Method

The calculations are performed on density functional theory (DFT) with Vienna ab initio package (VASP) [2]. The exchange-correlation interactions are describe by general gradient approximation of Perdew-Burke-Ernzerhof (GGA-PBE) [3]. The energy cutoff of plane wave functions are set to 500 eV. A 20 Å vacuum layer is used. The reciprocal space is sampled using a 4 × 4 × 1 point grid by Monkhorst-Pack K-points scheme. The structures are relaxed until the residual force on each atom is less than 0.01 eV $Å^{-1}$. The calculated lattice constants of MoN along x, y and z axes are 8.79 Å, 8.79 Å and 13.62 Å. The adsorption energies are calculated by the equation:

$$E_a = E_{Li_2S_x + substrate} - E_{Li_2S_x} - E_{substrate}$$

Where, the E_a, $E_{Li_2S_x + substrate}$, $E_{Li_2S_x}$ and $E_{substrate}$ represent the adsorption energy, the total energy of Li_2S_x species, the total energy of Li_2S_x and the total of the MoN substrates.

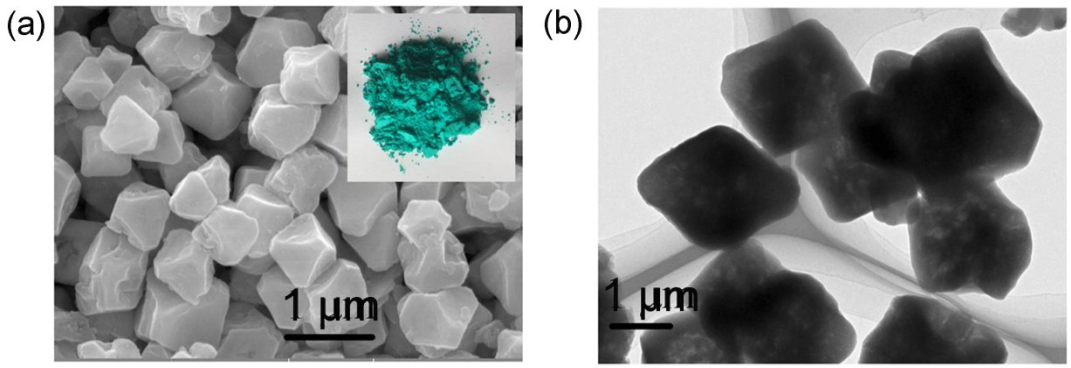

Figure S-1. (a) and (b): the as-prepared SEM and TEM image of NENU-5 POMOFs; the insert picture is the digital photos of NENU-5 POMOFs.

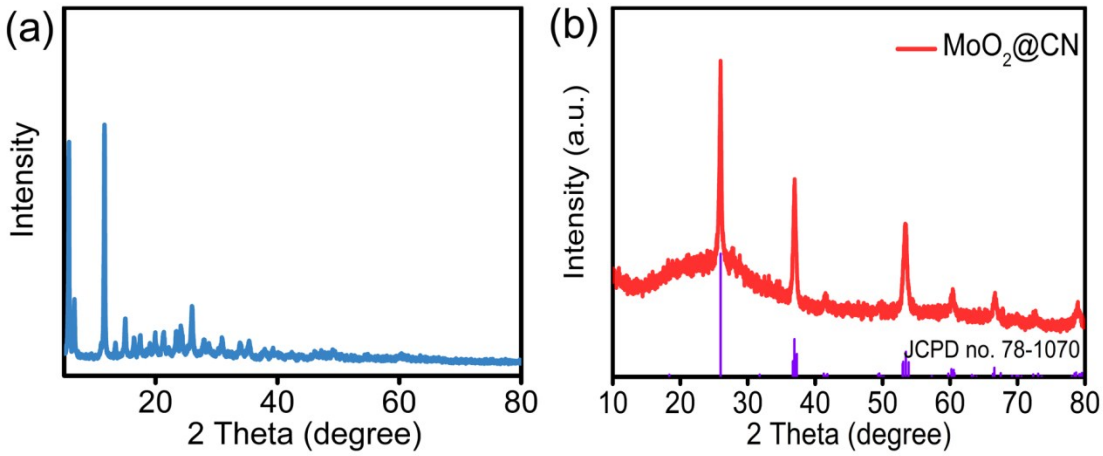

Figure S-2. a) XRD pattern of NENU-5 POMOFs and XRD pattern of MoO_2/CN.

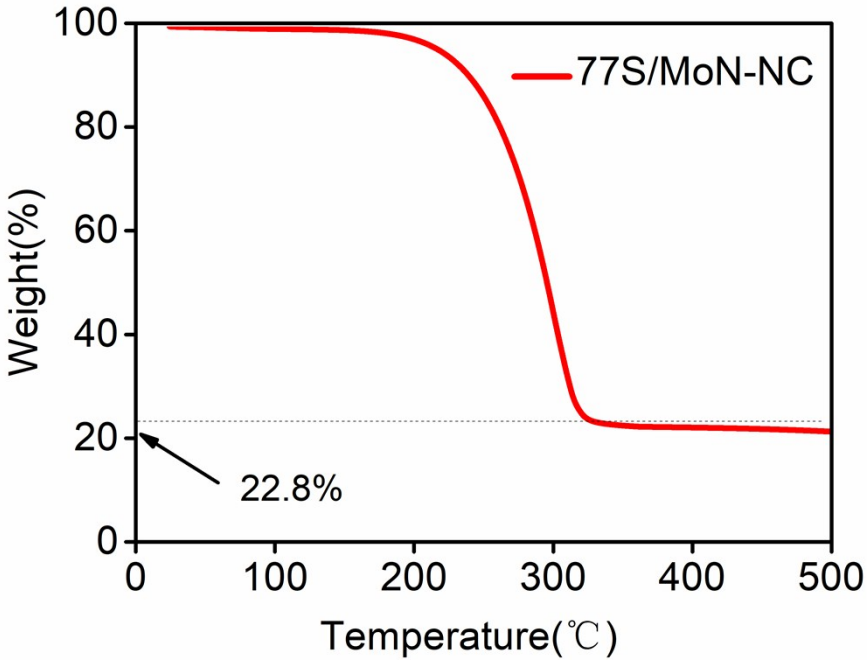

Figure S-3. Thermogravimetric curve of 77S/MoN-NC.

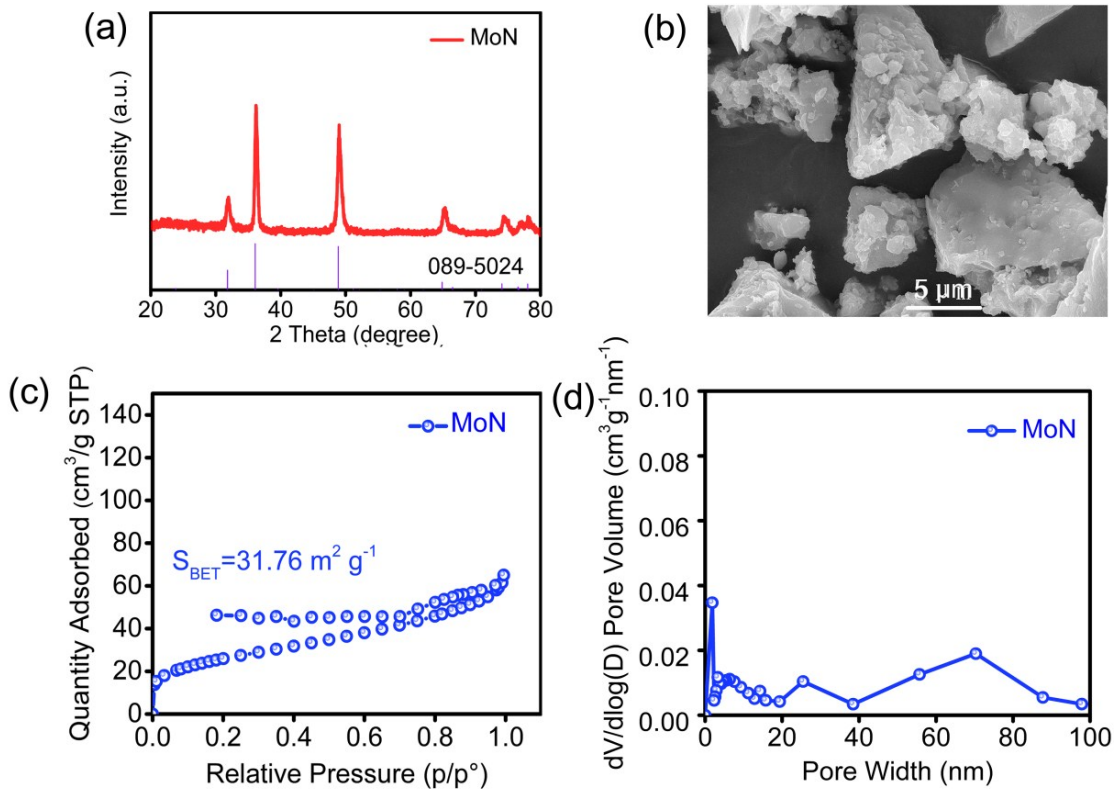

Figure S-4. a) XRD patterns; (b) SEM image; (c) N_2 adsorption-desorption isotherms isotherms, and (d) pore size distributions of the as-prepared MoN.

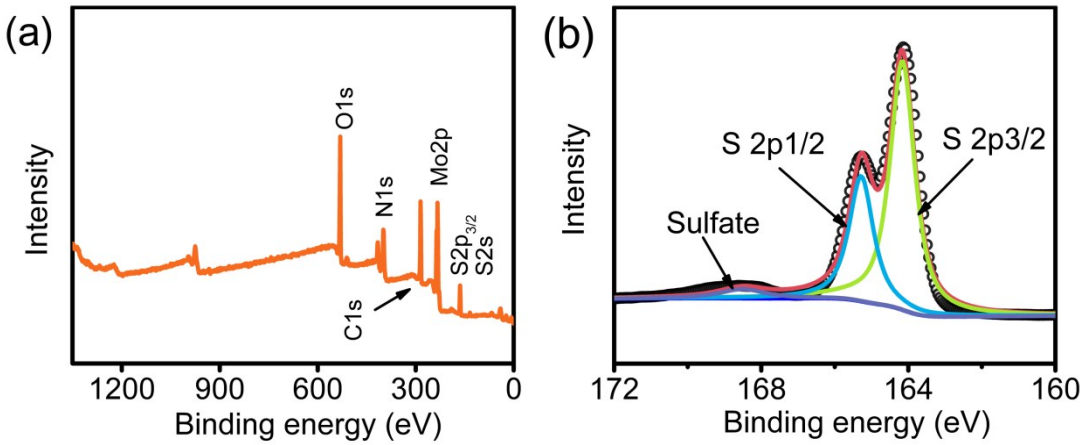

Figure S-5. a) The overview XPS spectrum of 77S/Mo-NC composites; (b) XPS spectra of S 2p for the 77S/Mo-NC composites.

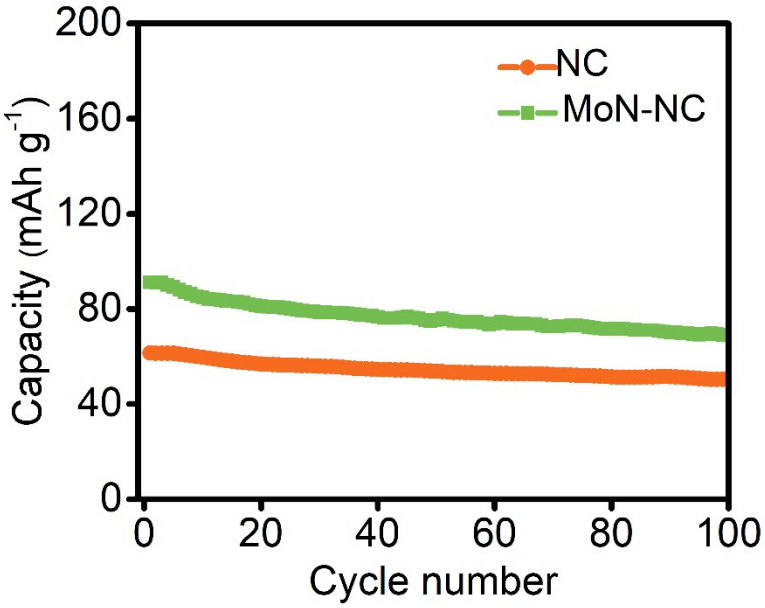

Figure S-6. Long-term cycling performance of the NC and MoN-NC electrodes. (current density= 837 mA g^{-1})

The maximum capacity that MoN nanoparticles was expected to contribute by their Li^+ intersection pseudo-capacitive behavior is calculated according to The specific capacity of MoN ×(MoN/S ratio of the 77S/MoN-NC cathode)

For example,

The specific capacity of MoN =86 mA h g^{-1},

MoN/S ratio of the NC/ MoN /S cathode = (0.23×0.11) / 0.77 = 0.032

The increased specific capacity of sulfur contributed by MoN in the 77S/MoN-NC cathode = 86×0.032 = 2.8 mA h g^{-1}.

The NC deliver more than 60 mA h g^{-1}, should because the pseudo-capacitive Li^+ storage behaviour. It should be noted that after the sulfur impregnation, the surface of carbon framework should be covered by the

sulfur, thus the electronic double layer capacitance (EDLC) of NC should be heavily discounted. Considering the Li^+ insertion-desertion redox reaction, the pseudo-capacitive-type capacity of MoN shall not be affected. But it only contributes less than 0.3% of overall capacity (2.8 mAh g^{-1} vs 934 mAh g^{-1} at 0.5 C).

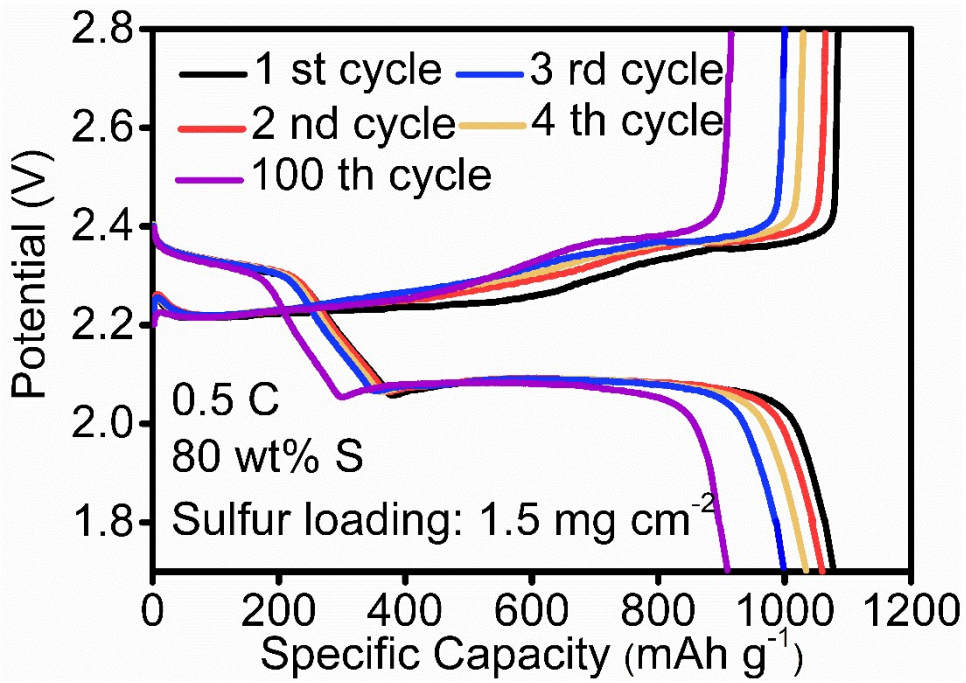

Figure S-7. Galvanostatic discharge-charge voltage profile at 0.5 C of 77S/MoN-NC composite.

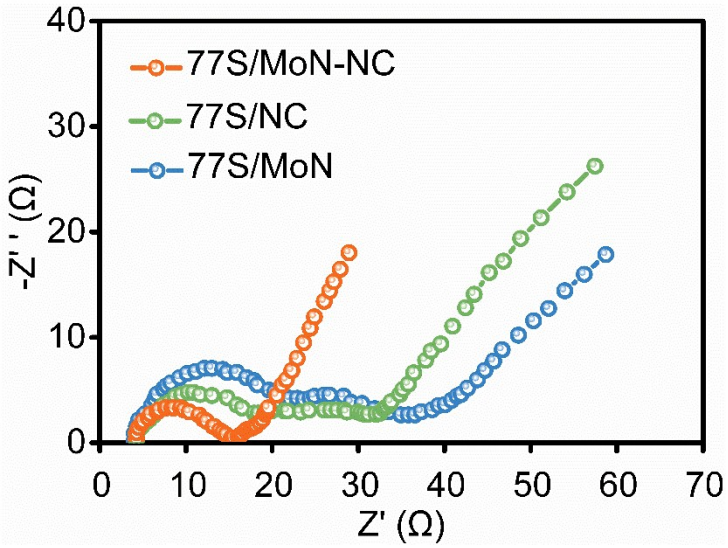

Figure S-8. EIS spectra of 77S/MoN-NC, 77S/MoN and 77S/NC after 200 cycles.

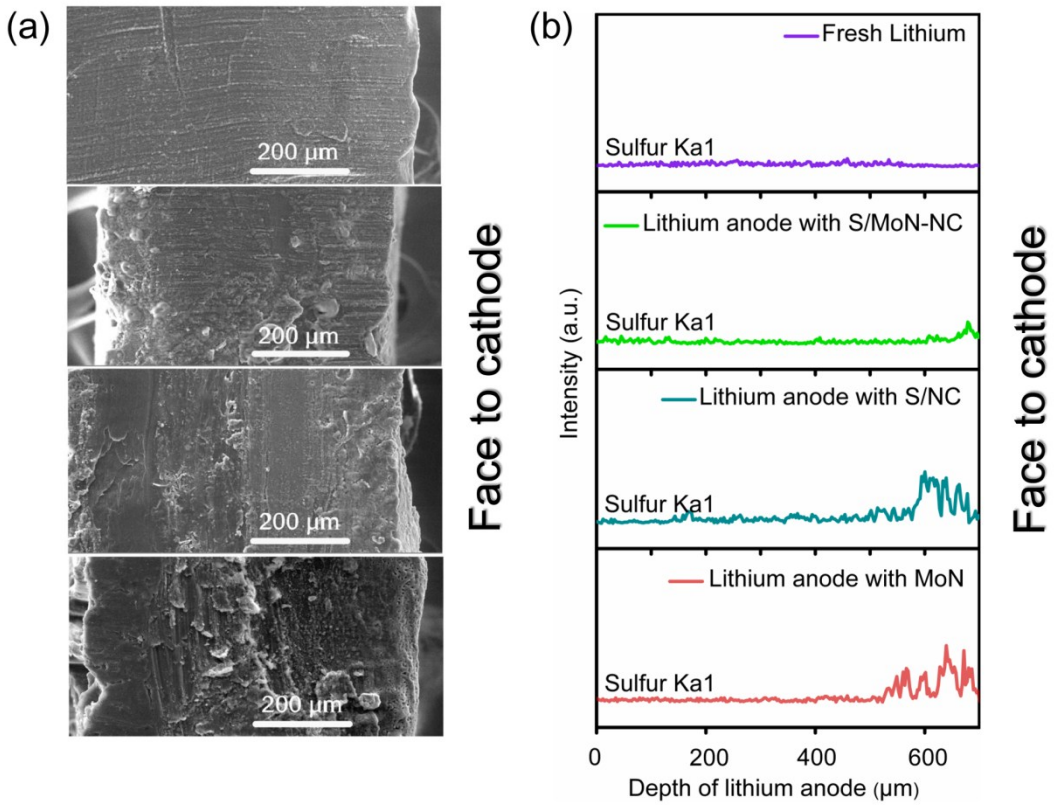

Figure S-9. a) The cross-section SEM images and b) the corresponding energy-dispersive X-ray spectroscopys (EDS) analysis of fresh lithium anode and the cross-section SEM images of lithium anode after 200 cycles combing with MoN-NC, MoN and NC.

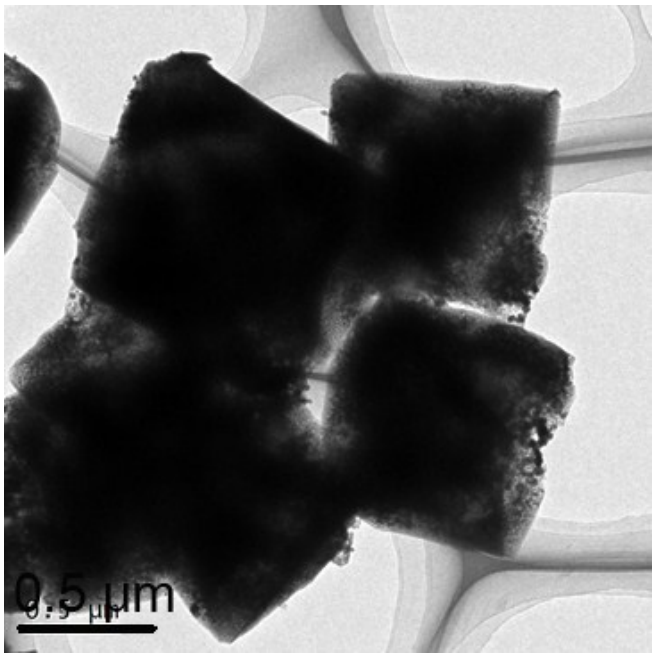

Figure S-10. Ex situ TEM image of 77S/Mo-NC cycles after 400 cycles.

Table S-1. Comparison of the cycling performance of this work with other previously reported metal compounds as sulfur host materials for Li-S batteries.

Ref.	Sulfur host	Sulfur weight (wt.%)	Sulfur loading	Current rate (C)	Cycle number	Capacity (mAh g^{-1})
This work	MoN-NC	77	6.5	0.5	200	597
4	Porous-Shell VN nanobubbles	78.2	5.7	0.33	200	563
5	WN		8	0.1	100	697
6	Porous Carbon Fibers/Vanadium Nitride Arrays	60	8.1	1	250	912
7	ACNF/CoS	50	7.5	0.5	100	701
8	CoO/Co@PCF	60	5.4	0.5	100	684
9	VN		6.8	0.5	200	563

References

(1) Wu, H. B.; Xia, B. Y.; Yu, L.; Yu, X.-Y.; Lou, X. W. D. Porous molybdenum carbide nano-octahedrons synthesized via confined carburization in metal-organic frameworks for efficient hydrogen production. Nature communications 2015, 6, 6512.

(2) Kresse, G.; Furthmüller, J. Efficiency of ab-initio total energy calculations for metals and semiconductors using a plane-wave basis set. Computational materials science 1996, 6 (1), 15-50.

(3) Perdew, J. P.; Chevary, J. A.; Vosko, S. H.; Jackson, K. A.; Pederson, M. R.; Singh, D. J.; Fiolhais, C. Atoms, molecules, solids, and surfaces: Applications of the generalized gradient approximation for exchange and correlation. *Physical Review B* **1992,** *46* (11), 6671.

(4) Ma, L.; Yuan, H.; Zhang, W.; Zhu, G.; Wang, Y.; Hu, Y.; Zhao, P.; Chen, R.; Chen, T.; Liu, J. Porous-shell vanadium nitride nanobubbles with ultrahigh areal sulfur loading for high-capacity and long-life lithium–sulfur batteries. Nano letters 2017, 17 (12), 7839-7846.

(5) Mosavati N, Salley S O, Ng K Y S. Characterization and electrochemical activities of nanostructured transition metal nitrides as cathode materials for lithium sulfur batteries[J]. Journal of Power Sources, 2017, 340: 210-216..

(6) Zhong, Y.; Chao, D.; Deng, S.; Zhan, J.; Fang, R.; Xia, Y.; Wang, Y.; Wang, X.; Xia, X.; Tu, J. Confining Sulfur in Integrated Composite Scaffold with Highly Porous Carbon Fibers/Vanadium Nitride Arrays for High-Performance Lithium–Sulfur Batteries. Advanced Functional Materials 2018, 28 (38), 1706391.

(7) Xu, H.; Manthiram, A. Hollow cobalt sulfide polyhedra-enabled long-life, high areal-capacity lithium-sulfur batteries. Nano Energy 2017, 33, 124-129.

(8) Ren, W.; Ma, W.; Umair, M. M.; Zhang, S.; Tang, B. CoO/Co-Activated Porous Carbon Cloth Cathode for High Performance Li–S Batteries. ChemSusChem 2018, 11 (16), 2695-2702.

(9) Ma, L.; Yuan, H.; Zhang, W.; Zhu, G.; Wang, Y.; Hu, Y.; Zhao, P.; Chen, R.; Chen, T.; Liu, J. Porous-shell vanadium nitride nanobubbles with ultrahigh areal sulfur loading for high-capacity and long-life lithium–sulfur batteries. Nano letters 2017, 17 (12), 7839-7846.